Article

Structure-Dependent Reactivity of Semiconducting Single-Walled Carbon Nanotubes with Benzenediazonium Salts

Condell D. Doyle, John-David R. Rocha, R. Bruce Weisman, and James M. Tour

J. Am. Chem. Soc., **2008**, 130 (21), 6795-6800 • DOI: 10.1021/ja800198t • Publication Date (Web): 03 May 2008

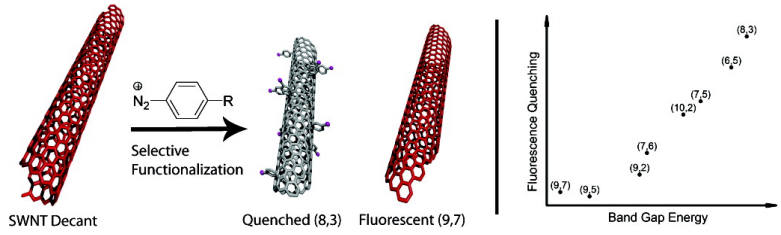

More About This Article

Additional resources and features associated with this article are available within the HTML version:

- Supporting Information
- Links to the 3 articles that cite this article, as of the time of this article download
- Access to high resolution figures
- Links to articles and content related to this article
- Copyright permission to reproduce figures and/or text from this article

View the Full Text HTML

J|A|C|S
ARTICLES

Published on Web 05/03/2008

Structure-Dependent Reactivity of Semiconducting Single-Walled Carbon Nanotubes with Benzenediazonium Salts

Condell D. Doyle,[†] John-David R. Rocha,[†,§] R. Bruce Weisman,*[,†] and James M. Tour*[,†,‡]

Departments of Chemistry and Mechanical Engineering and Materials Science, the R.E. Smalley Institute for Nanoscale Science and Technology, MS-222, and the Center for Biological and Environmental Nanotechnology, MS-63, Rice University, 6100 Main Street, Houston, Texas 77005

Received January 9, 2008; E-mail: tour@rice.edu; weisman@rice.edu

Abstract: The addition of diazonium salts to single-walled carbon nanotubes (SWCNTs) in aqueous surfactant suspensions quenches the intrinsic near-infrared fluorescence of semiconducting SWCNTs through sidewall chemical reactions. Spectrally resolved fluorescence spectroscopy of mixed SWCNT samples has been used to measure structure-dependent relative reactivities in the initial stages of these reactions. For several 4-substituted benzenediazonium salts, Ar−R (Ar = $N_2^+-C_6H_4$ and R = Cl, NO_2, OMe), reactivities at pH 10 were found to be greatest for SWCNTs having the largest band gaps. The magnitude of this band gap dependence varies according to the R-group of the salt, with R = OMe showing the strongest variation. For R = OH, acidification of the sample to pH 5.5 results in reversal of the structural trend, as smaller band gap SWCNTs show slightly greater reactivities. The derivatization reactions observed here proceed concurrently, although at different rates, for semiconducting and metallic SWCNT species. These results therefore provide insight into the difficulties of separating metallic and semiconducting SWCNTs through selective reaction schemes and underscore the need for fluorescence spectroscopy to be used in assessing semiconducting SWCNT reactions.

Introduction

Since the discovery of single-walled carbon nanotubes (SWCNTs), researchers have noted their remarkable chemical, structural, optical, and electrical properties.[1] SWCNTs exist in a variety of structural forms differing in diameter and chiral angle (indexed by a pair of integers (n,m)) and having metallic or semiconducting electronic properties. Statistically, a mixed sample of HiPco-derived SWCNTs will contain $^1/_3$ metallic and $^2/_3$ semiconducting species. The semiconducting subset contains a variety of band gaps that vary approximately inversely with nanotube diameter. Current practical SWCNT production methods result in significant structural polydispersity.[2–5] To facilitate the use of SWCNTs in optical and electronics applications, techniques for separating SWCNTs by structural type will be very valuable. Many reported separation attempts have exploited chemical reactivity differences among SWCNT types, but none of these methods have yielded structurally monodisperse products. Instead, only enrichment of metallic or semiconducting subpopulations has been found.[6–15]

In particular, prior research from this institution focused on covalent functionalization of SWCNTs by benzenediazonium salts.[16] This work described the nearly exclusive reaction of

[†] Department of Chemistry.
[‡] Department of Mechanical Engineering and Materials Science.
[§] Current address: National Renewable Energy Laboratory, MS-3216, 1617 Cole Blvd., Golden, Colorado 80401.

(1) Iijima, S.; Ichihashi, T. *Nature* **1993**, *363*, 603–605.
(2) Bachilo, S. M.; Strano, M. S.; Kittrell, C.; Hauge, R. H.; Smalley, R. E.; Weisman, R. B. *Science* **2002**, *298*, 2361–2366.
(3) Nikolaev, P.; Bronikowski, M. J.; Bradley, R. K.; Rohmund, F.; Colbert, D. T.; Smith, K. A.; Smalley, R. E. *Chem. Phys. Lett.* **1999**, *313*, 91–97.
(4) Bachilo, S. M.; Balzano, L.; Herrera, J. E.; Pompeo, F.; Resasco, D. E.; Weisman, R. B. *J. Am. Chem. Soc.* **2003**, *125*, 11186–11187.
(5) Kiang, C.-H.; Goddard, W. A., III.; Beyers, R.; Salem, J. R.; Bethune, D. S. *J. Phys. Chem.* **1994**, *98*, 6612–6618.
(6) Chattopadhyay, D.; Galeska, L.; Papadimitrakopoulos, F. *J. Am. Chem. Soc.* **2003**, *125*, 3370–3375.
(7) Samsonidze, G. G.; Chou, S. G.; Santos, A. P.; Brar, V. W.; Dresselhaus, G.; Dresselhaus, M. S.; Selbst, A.; Swan, A. K.; Unlu, M. S.; Goldberg, B. B.; Chattopadhyay, D.; Kim, S. N.; Papadimitrakopoulos, F. *Appl. Phys. Lett.* **2004**, *85*, 1006–1008.
(8) Krupke, R.; Hennrich, F.; von Lohneysen, H.; Kappes, M. M. *Science* **2003**, *301*, 344–347.
(9) Chen, Z. H.; Du, X.; Du, M. H.; Rancken, C. D.; Cheng, H. P.; Rinzler, A. G. *Nano Lett.* **2003**, *3*, 1245–1249.
(10) Dyke, C. A.; Stewart, M. P.; Tour, J. M. *J. Am. Chem. Soc.* **2005**, *127*, 4497–4509.
(11) An, L.; Fu, Q. A.; Lu, C. G.; Liu, J. *J. Am. Chem. Soc.* **2004**, *126*, 10520–10521.
(12) Balasubramanian, K.; Sordan, R.; Burghard, M.; Kern, K. *Nano Lett.* **2004**, *4*, 827–830.
(13) Zheng, M.; Jagota, A.; Semke, E. D.; Diner, B. A.; McClean, R. S.; Lustig, S. R.; Richardson, R. E.; Tassi, N. G. *Nat. Mater.* **2003**, *2*, 338–342.
(14) Zheng, M.; Jagota, A.; Strano, M. S.; Santos, A. P.; Barone, P. W.; Chou, S. G.; Diner, B. A.; Dresselhaus, M. S.; McIean, R. S.; Onoa, G. B.; Samsonidze, G. G.; Semke, E. D.; Usrey, M. L.; Walls, D. J. *Science* **2003**, *302*, 1545–1548.
(15) Huang, X.; Mclean, R. S.; Zheng, M. *Anal. Chem.* **2005**, *77*, 6225–6228.
(16) Strano, M. S.; Dyke, C. A.; Usrey, M. L.; Barone, P. W.; Allen, M. J.; Shan, H.; Kittrell, C.; Hauge, R. H.; Tour, J. M.; Smalley, R. E. *Science* **2003**, *301*, 1519–1522.

Scheme 1. Functionalization of Surfactant-Wrapped SWCNTs by Addition of 4-Substituted Benzenediazonium Salts at Basic pH

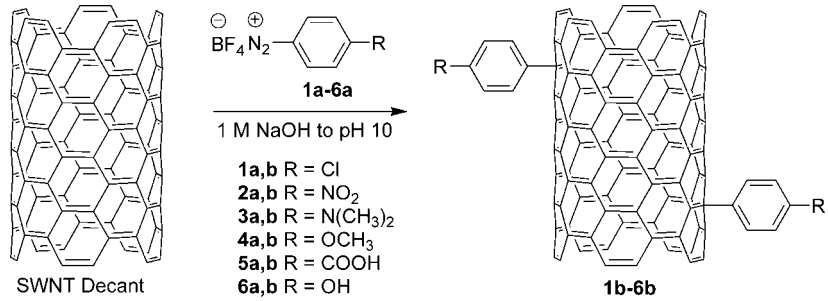

Table 1. Reaction Conditions for the Various SWCNT + Benzenediazonium Studies

experiment	surfactant	diazonium salt[a]	temp (°C)	pH	[DZ][b] (mM)
T1	Pluronic F-87	**1a**	5	10	4
T2	Pluronic F-87	**1a**	5	10	2
T3	SDBS	**1a**	20	10	4
T4	SDBS	**1a**	11	10	4
T5	SDBS	**1a**	11	4	4
T6	SDBS	**2a**	11	10	4
T7	SDBS	**3a**	11	10	4
T8	SDBS	**4a**	11	10	4
T9	SDBS	**5a**	11	10	4
T10	SDBS	**6a**	11	10	4
T11	SDBS	**6a**	11	5.5	4
T12	SDBS	**6a**	45	5.5	4

[a] See notations in Scheme 1. [b] Diazonium salt concentration.

these salts with metallic rather than semiconducting SWCNT species, as deduced mainly from bleaching of absorption spectra.[16] The mechanism for this system has recently been delineated by Strano and co-workers using solution phase resonance Raman spectroscopy.[17] This work also focused on the (*n*,*m*)-dependent reactivities among semiconductor types and found that the larger diameter SWCNTs reacted much more rapidly than the smaller diameter nanotubes.[18,19]

The optical properties of SWCNTs are dominated by sharp maxima in the electronic densities of states arising from the one-dimensional character of the π-electron states.[20] A mixed sample of SWCNTs with an average diameter near 1 nm shows three distinct optical absorption bands: the E_{11}^{M} transitions from ~450 to 550 nm arising from metallic species, the E_{22}^{S} semiconducting transitions from ~550 to 900 nm, and the E_{11}^{S} semiconducting transitions from ~900 to 1600 nm. Since the 2002 assignment of SWCNT spectroscopic transitions to specific (*n*,*m*) structural species in samples containing individually suspended nanotubes,[2] it has become feasible to study structure-dependent chemical reactions of SWCNTs through changes in their optical spectra.[16,21,22] Although both absorption and fluorescence spectra can be interpreted as superpositions of underlying (*n*,*m*) components, fluorescence spectra are more readily resolved because there is no broad background to subtract and overlapping emission features can be dissected by using different excitation wavelengths. Fluorescence also provides much higher sensitivity, allowing the study of dilute SWCNT samples. When SWCNTs undergo sidewall derivatization reactions, their absorption features are bleached and their fluorescence emissions are quenched. However, because nanotube excitons are mobile and can visit approximately 10^4 sites during their natural lifetime,[23] chemical perturbations can be detected far more sensitively by fluorescence quenching than by absorption bleaching. This permits reactions to be monitored at early stages of product formation. Nevertheless, fluorescence is restricted to semiconducting species; metallic nanotubes must be detected through their absorptions.

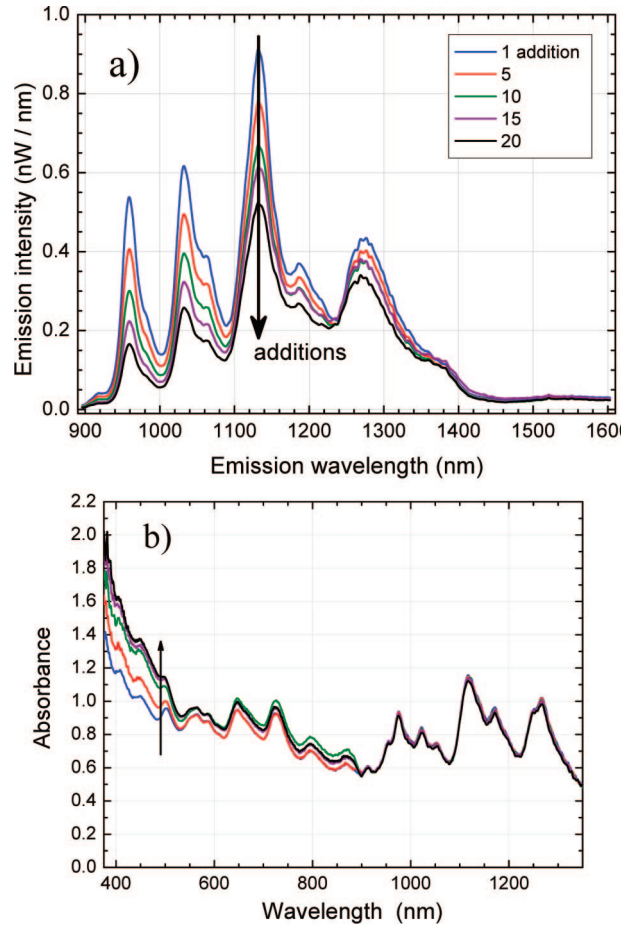

Figure 1. (a) Emission spectra following 20 μL additions of 4-chlorobenzenediazonium salt (**1a**) to 25 mL of SWCNT Pluronic suspension (T1). Spectra were measured after 1, 5, 10, 15, and 20 injections. (b) Absorption spectra of the same sample. The arrow points in the direction of increasing numbers of injections.

(17) Usrey, M. L.; Lippmann, E. S.; Strano, M. S. *J. Am. Chem. Soc.* **2005**, *127*, 16129–16135.
(18) Nair, N.; Usrey, M. L.; Kim, W.; Braatz, R. D.; Strano, M. S. *Anal. Chem.* **2006**, *78*, 7689–7696.
(19) Nair, N.; Kim, W. J.; Usrey, M. L.; Strano, M. S. *J. Am. Chem. Soc.* **2007**, *129*, 3946–3954.
(20) Saito, R.; Dresselhaus, G.; Dresselhaus, M. S. *Physical Properties of Carbon Nanotubes*; Imperial College Press: London, 1998.
(21) Strano, M. S.; Huffman, C. B.; Moore, V. C.; O'Connell, M. J.; Haroz, E. H.; Hubbard, J.; Miller, M.; Rialon, K.; Kittrell, C.; Ramesh, S.; Hauge, R. H.; Smalley, R. E. *J. Phys. Chem. B* **2003**, *107*, 6979–6985.
(22) O'Connell, M. J.; Eibergen, E. E.; Doorn, S. K. *Nat. Mater.* **2005**, *4*, 412–418.

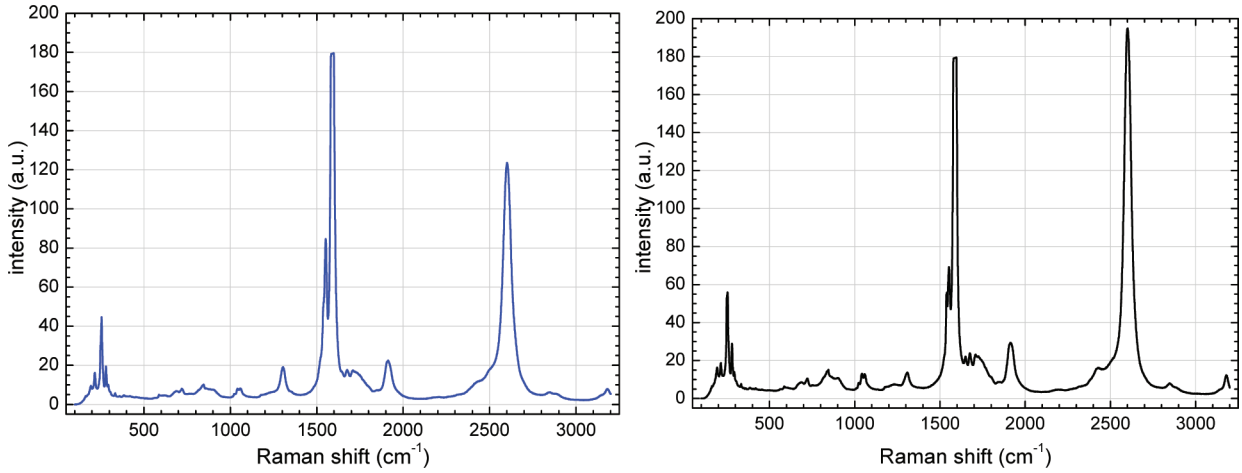

Figure 2. Raman spectra for SWCNT buckypaper prepared from SWCNTs before (left frame) and after (right frame) solution phase reaction with a diazonium salt (T1). The excitation laser was at 633 nm.

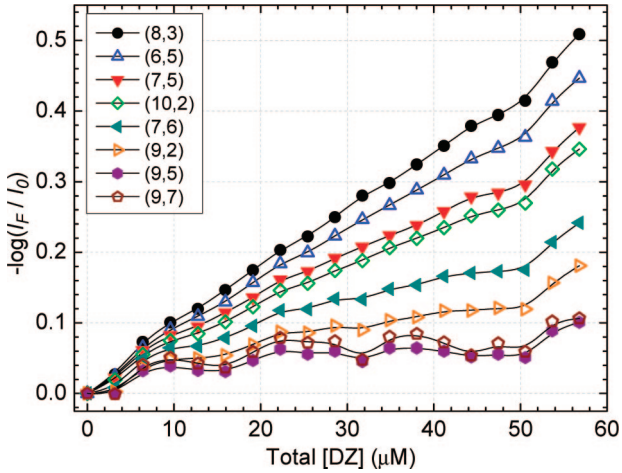

Figure 3. Fluorescence quenching plots for eight different semiconducting SWCNT species in Pluronic suspension (T1) following 20 μL additions of 4-chlorobenzene diazonium salt (**1a**) solution.

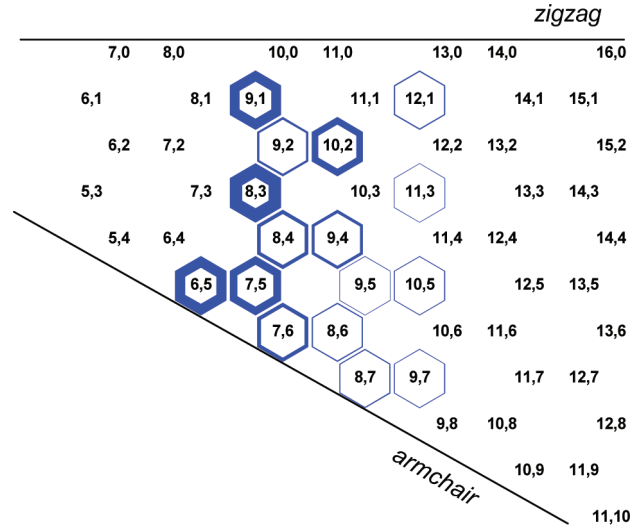

Figure 4. Modified Bachilo−Weisman plot illustrating relative reactivities of 4-chlorobenzenediazonium (**1a**, T1) for different semiconducting (*n*,*m*) species in aqueous Pluronic suspension. The thickness of each hexagonal border is proportional to the relative reactivities of the enclosed (*n*,*m*) species (not the abundances of the species).

We report here fluorescence-based studies of (*n*,*m*)-dependent reactivities of semiconducting SWCNTs toward a range of benzenediazonium salts. Strong kinetic variations with nanotube structure, diazonium species, surfactant, and pH are found. These results lead to a better understanding of the dominant reaction mechanisms in this important system and suggest future approaches to attaining effective bulk separation of nanotube species.

Experimental Section

Sample Preparation. All SWCNTs were produced by the HiPco process (Carbon Nanotechnology Laboratory, Rice University).[3] Raw or purified SWCNTs were dispersed in aqueous solutions of 1 wt % sodium dodecylsulfate (SDS), sodium dodecylbenzenesulfonate (SDBS), or Pluronic F-87 (a nonionic poly(ethylene glycol)/poly(propylene glycol)/poly(ethylene glycol) triblock copolymer with the average molecular weight of 7700, BASF mat. no. 30085465) via methods previously described.[24] The resulting suspensions were then adjusted to the desired pH levels by addition of 1 N NaOH or 1 N HCl. In experiments that exceeded 6 h, a fresh solution of diazonium salt was prepared every 6 h. The diazonium salts were stored in powder form under nitrogen at −20 °C until used. Diazonium solutions were prepared in a scintillation vial, wrapped in foil, and kept cold in the temperature-regulated bath that held the reaction vessels.

Data Collection. Two-dimensional fluorescence emission data were collected using a J-Y Spex Fluorolog 3-211 spectrofluorometer equipped with a liquid-N_2-cooled InGaAs detector.[2] Scans were obtained using excitation intervals of 3 nm with a 10 nm spectral slit width and emission intervals of 2 nm with a 6 nm slit width. Reaction runs were monitored using one-dimensional fluorescence emission spectra acquired with 661 nm laser excitation in an NS1 NanoSpectralyzer (Applied NanoFluorescence, LLC). Typical spectra were the average of 10 to 25 acquisitions of 0.5 s. All emission intensities were corrected for the wavelength dependent instrumental sensitivities. Visible and near-IR absorbance data

(23) Cognet, L.; Tsyboulski, D.; Rocha, J.-D. R.; Doyle, C. D.; Tour, J. M.; Weisman, R. B. *Science* **2007**, *316*, 1465–1468.

(24) O'Connell, M.; Bachilo, S. M.; Huffman, C. B.; Moore, V.; Strano, M. S.; Haroz, E.; Rialon, K.; Boul, P. J.; Noon, W. H.; Kittrell, C.; Ma, J.; Hauge, R. H.; Weisman, R. B.; Smalley, R. E. *Science* **2002**, *297*, 593–596.

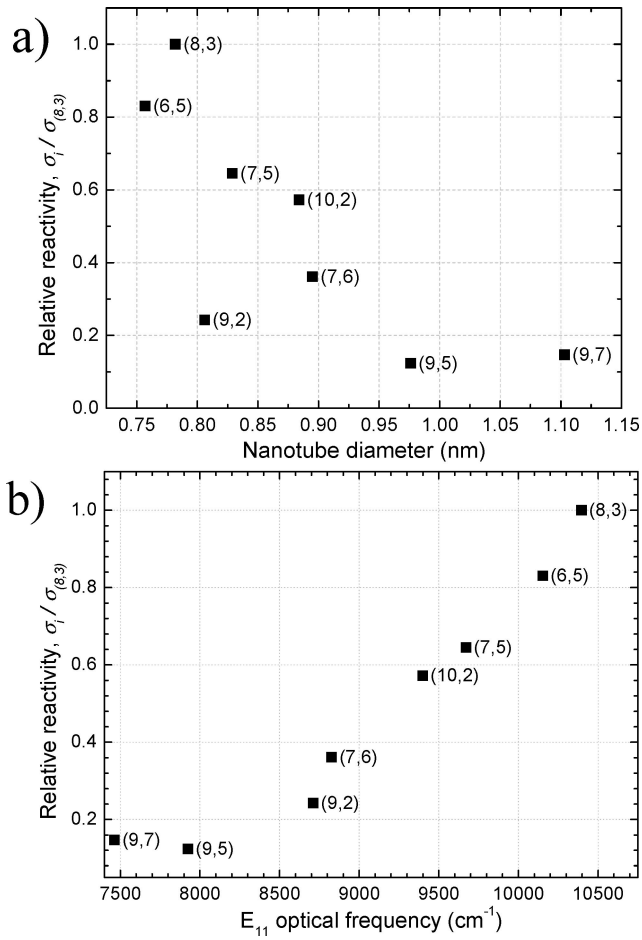

Figure 5. Plot of relative reactivities (RRs) versus (a) nanotube diameters and (b) $E_{11}{}^{s}$ fluorescence frequencies for the eight (*n*,*m*) SWCNT species studied in reaction with 4-chlorobenzenediazonium (**1a**, T1).

(400–1600 nm) were collected on the NanoSpectralyzer (10 spectral averages, 0.5 s acquisition time). Raman spectra of solid SWCNT samples were collected before and after reaction using both 633 and 785 nm excitation on a Raman microscope (RM 2000, Renishaw Inc.).

In a typical experiment (Scheme 1), 25 mL of decanted SWCNT/surfactant suspension and a stir bar were added to a round-bottom flask and then placed in a circulating coolant bath (5 °C for Pluronic samples and 11 °C for SDBS samples) or left at room temperature.

We added 20 to 40 aliquots, spaced by 1 h intervals, of ~4 mM aqueous solutions of 4-substituted benzenediazonium salts, Ar-R ($Ar = N_2{}^{+}-C_6H_4$, R = Cl, NO_2, OMe, $N(CH_3)_2$, COOH, or OH). Each aliquot had a volume of 20 μL. The reaction conditions utilized are summarized in Table 1.

We removed a 400 μL sample of the reaction solution 1 h after each addition. It was allowed to warm to room temperature for spectrofluorimetric analysis and then returned to the reaction vessel. Since this procedure can lead to experiment runs in excess of 40 h, a short series of experiments were performed utilizing larger (200 μL) reactant additions every hour for 6 h. A control experiment using sodium tetrafluoroborate salt addition was also performed. This gave no fluorescence quenching. The decant SWCNT samples that were used here had concentrations near 30 mg/L, but our results were not sensitive to this concentration.

Results and Discussion

A representative set of experimental fluorescence emission spectra are presented in Figure 1. The emission intensity decreases markedly following addition of 4-chlorobenzenediazonium salt (**1a**) and continues to decrease with subsequent additions of the reactant.

However, during the course of the reactions, there was little change in the sample's absorption spectrum in the region of prominent semiconductor $E_{11}{}^{s}$ transitions (900 to 1350 nm, Figure 1b). Although the visible absorption spectrum shows an increasing background component (likely from an azo dye formed as a reaction byproduct), the spectral structure near 500 nm is noticeably reduced, indicating derivatization of metallic SWCNTs in the sample.

A comparison of solid state Raman spectra measured before and after reaction is presented in Figure 2. Considering the sampling uncertainties arising in such solid phase measurements,[10] the two spectra show only minor differences in the primary areas of interest: the radial breathing mode region below 350 cm^{-1}, the D-band region near 1300 cm^{-1}, and the G-band region near 1590 cm^{-1}. The similarity of D/G ratios confirms that the extent of sidewall derivatization is very limited compared to the earlier study of Strano et al.[16]

The fluorescence quenching shown in Figure 1a is attributed to nonradiative exciton recombination at sites of localized perturbation to the semiconducting nanotube's π-electron system.[23] These may arise from (1) chemical reaction of SWCNT species with the diazonium salt or (2) charge transfer complex formation on the surface of the SWCNT. It has been shown that covalent reaction with a single diazonium salt molecule quenches exciton emission from a ~90 nm segment of a SWCNT.[23] As the SWCNT is further functionalized, the extent of quenching increases until the fluorescence intensity drops below detectable limits.

Using the (*n*,*m*) assignment of Bachilo et al.,[2] emission from specific semiconducting species can be analyzed separately. One can compare the various (*n*,*m*) species by plotting the fractional decreases in emission intensity vs concentration of diazonium reactant added, according to the equation

$$-\log\left(\frac{I_F}{I_0}\right) = \sigma_i[DZ] \qquad (1)$$

where I_F and I_0 are the fluorescence intensity after addition of a reactant and the initial intensity, respectively; σ is a parameter representing the extent of the quenching reaction; and [DZ] is the molar concentration of the diazonium salt. Fluorescence intensities of different (*n*,*m*) SWCNT species were deduced from the amplitudes of spectral peaks dominated by those species. Based on our previous study, we assume that the relative fluorescence quenching per reaction event is constant among the different species.[23]

The quenching of eight semiconducting SWCNT species was analyzed. These (*n*,*m*) structures, (8,3), (6,5), (7,5), (10,2), (7,6), (9,2), (9,5), and (9,7), were chosen because they are spectrally distinct in emission or nearly resonant in absorption with the excitation laser wavelength. Linear least-squares fitting of the data in Figure 3a yielded a σ_i value for each designated (*n*,*m*) species. We then took the ratios $\sigma_i/\sigma_{(8,3)}$ to obtain the relative reactivities shown as cell border thicknesses in Figure 4.

To help deduce the reaction mechanism, it is important to determine whether the large differences in relative reactivities are governed by nanotube diameter, chiral angle, or E_{11} optical band gap. Figure 4 clearly shows an absence of significant chiral angle dependence, letting us rule out that parameter. Distinguishing between diameter and optical band gap as governing factors is more difficult, however, because the two quantities

Scheme 2. Diazoanhydride formation under Basic Conditions, According to the Gomberg−Bachmann Mechanism[27]

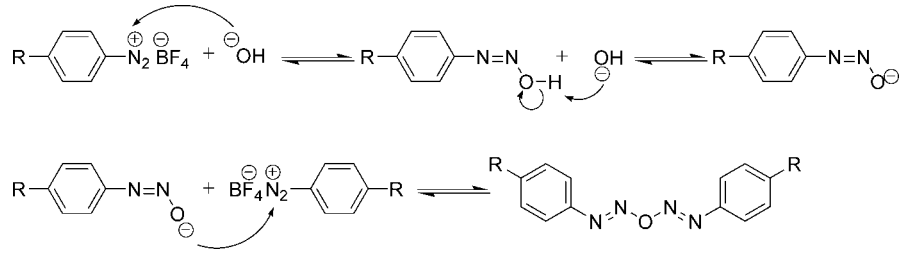

are closely linked. We have therefore prepared separate plots of relative reactivity as a function of diameter and band gap (Figure 5) and compared the R^2 values of the respective linear best fits. We found the correlation with optical band gap to be stronger, implying that HOMO–LUMO differences play a more important role in the reaction than pyramidalization effects or strain associated with nanotube curvature.[25,26] Figure 5b shows the nearly linear relationship between $\sigma_i/\sigma_{(8,3)}$ and optical transition frequency, with the larger E_{11} frequencies associated with higher reactivities.

In the 2003 study of SWCNT/diazonium reactions, which observed selective bleaching of metallic SWCNT absorption transitions, the mechanism of selective functionalization was deduced to involve injection of electrons from the metallic SWCNTs into the diazonium salt.[10,16] This mechanism would imply that the semiconducting SWCNT species with smaller band gaps would react more readily than those with larger band gaps. However, the results shown in Figure 5b reveal the opposite trend. An alternative mechanism can be considered under the Gomberg−Heys conditions (basic pH) used in this work.[27] In this model the electron-deficient diazonium salt becomes an electron-rich diazotate that reacts with another molecule of diazonium salt to yield the diazoanhydride (Scheme 2).

This electron-rich anhydride could preferentially form charge transfer complexes with the larger band gap, electron-poor SWCNTs. While physisorbed to the surface of the SWCNT, the complexed anhydride could then cleave to form an aryl free radical that attacks the SWCNT, forming a covalently bonded sidewall adduct.[28,29] This suggested mechanism is consistent with the reactivity pattern found in Figure 5b.

Because the proposed mechanism associates the diazoanhydride species with (n,m)-dependent reactivities, it predicts that greater reaction selectivity will occur for diazonium salts in which the R group (Scheme 1) more strongly promotes diazoanhydride formation. To test this hypothesis, we have measured relative reactivities for a variety of benzenediazonium salts. The results for five such reactants are plotted in Figure 6.

The observed trend in reactive selectivity is 4-methoxy (**4a**) > 4-dimethylamino (**3a**) > 4-chloro (**1a**) > 4-nitro (**2a**) > 4-carboxy (**5a**), whereas the trend expected from the electron-donating ability of the R groups would be 4-dimethylamino > 4-methoxy > 4-chloro > 4-carboxy > 4-nitro. We suggest that the reduced reactivity of 4-dimethylamino species may reflect steric hindrance from its two methyl groups. The 4-carboxy species shows a much lower reactivity and a very weak opposite

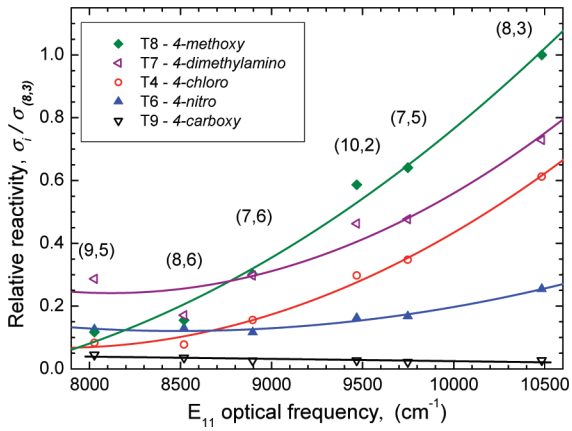

Figure 6. Relative reactivities vs optical emission frequency, measured for various diazonium salts at 11 °C. See Scheme 1 and Table 1 for T4, T6−T9 designations.

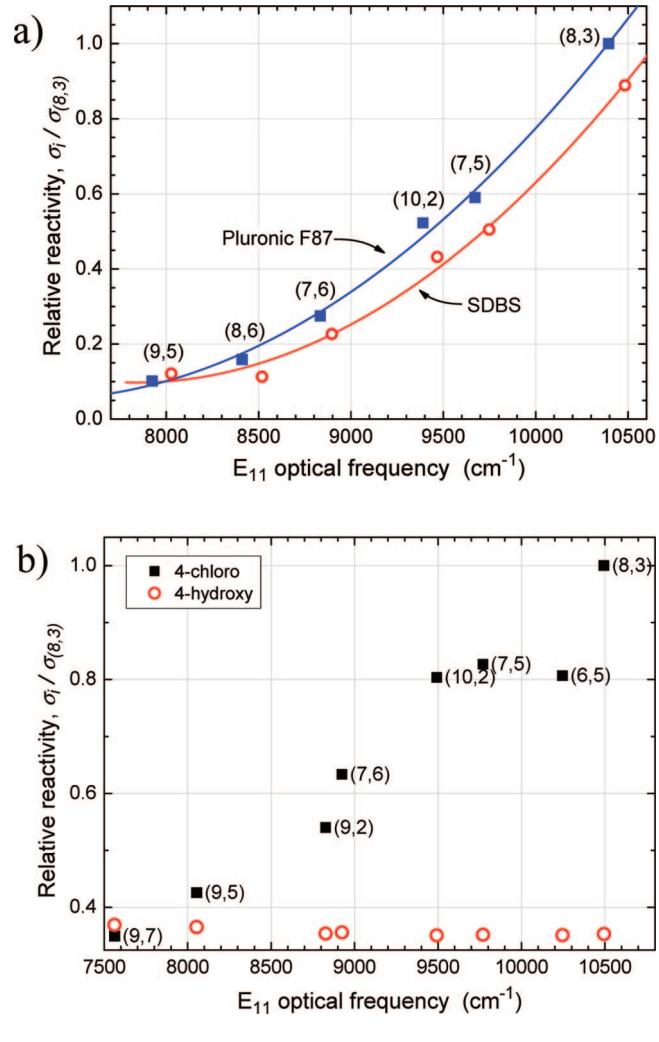

Figure 7. (a) Comparison of relative reactivities for reactions in Pluronic F-87 (T1) versus SDBS (T4). Data have been normalized to the (8,3) Pluronic point. (b) Comparison between 4-chloro (**1a**, T5) and 4-hydroxy (**6a**, T11) reactivities in acidic conditions.

variation with optical band gap. This can be attributed to the fact that it forms an ionic anhydride that may have limited access to the nonpolar micellar environment of the SWCNT. If our explanations account for the two exceptions, then the proposed mechanism is consistent with the observed reactivity trends. We note that the patterns of relative reactivities were essentially independent of diazonium salt concentration within the range 2−4 mM.

The surfactant also plays a role in the rate of SWCNT functionalization. As shown in Figure 7a, we find somewhat higher reaction rates for SWCNTs suspended in F87-Pluronic than those for SWCNTs in SDBS. This difference may be due to weaker and more permeable SWCNT wrapping by the highly disordered polymer coating as compared to SDBS micellar structures. The Pluronic coating would then allow the diazonium species to interact more readily with the SWCNT surface, facilitating functionalization. The same structure-dependent reactivity trends were found using SDS and SDBS surfactants under our standard reaction conditions (pH 10 and 11 °C).

We also investigated the effects of pH for two diazonium salts. When the 4-chloro (**1a**) salt was reacted at pH 4 rather than under basic conditions, we observed the same trend (reactivity increasing strongly with increasing band gap). By contrast, the dependence of 4-hydroxy (**6a**) salt reactivities on band gap reversed when the reaction was run at pH 5.5 rather than 10. Under the acidic conditions, the smallest band gap species showed reactivities slightly greater (∼5%) than the largest band gap species. These results are shown in Figure 7b. Our acidic 4-hydroxy findings are consistent with the recent report by Strano and co-workers[19] in which absorption spectra revealed the preferential reactivity of this diazonium salt with small band gap semiconducting SWCNTs.

Conclusions

Near-IR fluorescence spectroscopy has been applied to study the structure-dependent initial reactivities of semiconducting SWCNTs with a series of benzenediazonium salts. For most of these 4-substituted benzenediazonium salts, reactivities are greatest for SWCNTs having the largest band gaps, although weak opposite dependencies were found for the 4-hydroxy salt under acidic conditions and for the 4-carboxy species. We also found that reactivities were somewhat greater for SWCNTs suspended in Pluronic F-87 instead of SDBS. We propose that the dominant mechanism of the benzenediazonium reaction involves the formation of an electron-rich diazoanhydride, which preferentially complexes with large band gap SWCNTs.

We note that metallic SWCNT species are known to be more reactive than semiconducting SWCNTs.[16] Nevertheless, the reactions of semiconducting species observed here proceed concurrently with the reactions of metallic species; fluorescence spectroscopy is needed to detect the perturbations of the semiconductor sidewalls at low reactant concentrations. This explains why separations based in Scheme 1, which were initially thought to selectively functionalize metallic nanotubes,[16] were found to produce mixed products.[10] It seems likely that different reaction mechanisms are dominant in the reactions of diazonium salts with metallic versus semiconducting SWCNTs. The structure-sensitive nanotube reactions studied here may prove useful for enriching a SWCNT sample in large or small band gap semiconducting species.

Acknowledgment. We thank Drs. Dustin James, Dmitry Kosynkin, Sergei Bachilo, Howard Schmidt, and Prof. Paul Engel for helpful suggestions. C.D.D. and J.M.T. received financial support for this work from the NASA URETI TiiMs project and the DOE grant DE-FC36-05GO15073. J.-D.R.R. and R.B.W. acknowledge support from the National Science Foundation Chemistry Division (CHE-0314270), the NSF Center for Biological and Environmental Nanotechnology (EEC-0647452), the Welch Foundation (C-0807), and NASA (JSC-NNJ06HC25G). J.-D.R.R. also thanks the Rice-Houston AGEP program (NSF Cooperative HRD-0450363) for partial support.

JA800198T

(25) Haddon, R. C. *Science* **1993**, *261*, 1545–1550.
(26) Niyogi, S.; Hamon, M. A.; Hu, H.; Zhao, B.; Bhowmik, P.; Sen, R.; Itkis, M. E.; Haddon, R. C. *Acc. Chem. Res.* **2002**, *35*, 1105–1113.
(27) Smith, M. B.; March, J. *March's Advanced Organic Chemistry: Reactions, Mechanisms, and Structure*, 5th ed.; Wiley-Interscience: New York, 2001; p 929.
(28) Ruchardt, C.; Merz, E. *Tetrahedron Lett.* **1964**, 2431–2436.
(29) Eliel, E. L.; Saha, J. G.; Meyerson, S. *J. Org. Chem.* **1965**, *30*, 2451.